Molecular Modeling of the Short-Side-Chain Perfluorosulfonic Acid Membrane

Stephen J. Paddison*

Department of Chemistry and Materials Science, University of Alabama in Huntsville, Huntsville, Alabama 35899

James A. Elliott*

Department of Materials Science and Metallurgy, University of Cambridge, Pembroke Street, Cambridge, CB2 3QZ, UK

Received: May 11, 2005; In Final Form: June 30, 2005

Presented here is a first principles based molecular modeling investigation of the possible role of the side chain in effecting proton transfer in the short-side-chain perfluorosulfonic acid fuel cell membrane under minimal hydration conditions. Extensive searches for the global minimum energy structures of fragments of the polymer having two pendant side chains of distinct separation (with chemical formula: $CF_3CF(O(CF_2)_2SO_3H)(CF_2)_nCF(O(CF_2)_2SO_3H)CF_3$, where $n = 5$, 7, and 9) with and without explicit water molecules have shown that the side chain separation influences both the extent and nature of the hydrogen bonding between the terminal sulfonic acid groups and the number of water molecules required to transfer the proton to the water molecules of the first hydration shell. Specifically, we have found that fully optimized structures at the B3LYP/6-311G** level revealed that the number of water molecules needed to connect the sulfonic acid groups scaled as a function of the number of fluoromethylene groups in the backbone, with one, two, and three water molecules required to connect the sulfonic acid groups in fragments with $n = 5$, 7, and 9, respectively. With the addition of explicit water molecules to each of the polymeric fragments, we found that the minimum number of water molecules required to effect proton transfer also increases as the number of separating tetrafluoroethylene units in the backbone is increased. Furthermore, calculation of water binding energies on CP-corrected potential energy surfaces showed that the water molecules bound more strongly after proton dissociation had occurred from the terminal sulfonic acid groups independent of the degree of separation of the side chains. Our calculations provide a baseline for molecular results that can be used to assess the impact of changes of polymer chemistry on proton conduction, including the side chain length and acidic functional group.

Introduction

Polymeric materials that function as the critical electrolyte and electrode separator in proton exchange membrane (PEM) fuel cells exhibit a nano-phase-separated morphology when hydrated. However, only at high degrees of hydration are the currently available state-of-the-art PEMs able to conduct protons through the membrane at sufficiently high rates for successful operation of direct hydrogen fuel cells.[1] These power sources are deemed to possess the potential to lead to considerable energy savings, energy security, and air quality improvements through a wide range of modular power applications subject to the advent of improved materials (membranes, catalysts, etc).[2] Hence, the development of PEMs which operate at high temperature (i.e. > 100 °C) and low humidity conditions (thus without requiring pressurization of the system) and exclusively transport protons is widely regarded as an important research and development requirement for PEM fuel cell technology.

The design and synthesis of new membranes possessing improved performance characteristics (along with decreased manufacturing costs) will require a fundamental, molecular-based understanding of the mechanisms of proton and water transport as a function of membrane hydration, morphology, and polymer chemistry.[3] This information cannot come from experimental investigations alone, but will require knowledge of how membrane morphology and chemical composition affect the transport of both protons and water in the PEM through multiscale modeling that bridges many distinct time and length scales, connecting the equilibrium conformational structure of a membrane and its general composition to molecular processes including proton dissociation, transfer, and diffusion, and hydrogen bonding, distribution, and diffusion of water. This work seeks to contribute to this goal through a first principles based investigation into the ingredients of proton conduction in the short-side-chain perfluorosulfonic acid (PFSA) membrane at minimal hydration.

Interest in the mechanisms of proton conduction is, of course, not restricted to polymeric ionomers, as proton transfer and transport feature importantly in the function of many different chemical and biological systems.[4,5] Proton transport continues to be extensively studied both experimentally and theoretically in a variety of materials and diverse media[6] including (most importantly) water,[7−11] mixed aqueous solutions (i.e. aqueous CH_3OH[12]), acids,[13] solids[14,15] (e.g. oxides,[16] phosphates,[17] sulfates[18]) transmembrane proteins[19−21] (i.e. proton channels[22] and pumps[23]), carbon nanotubes,[24] and PEMs.[25−32] Clearly, an

* Correspondence may be addressed to either author. E-mail: paddison@matsci.uah.edu or jae1001@cam.ac.uk.

10.1021/jp0524734 CCC: $30.25
Published on Web 07/29/2005

understanding of both the common (i.e. in the formation of a continuous network of dynamical hydrogen bonds and the excess protonic charge following the center of symmetry of the hydrogen bond coordination) and distinct features in the molecular details of proton movement in these systems will prove helpful in the development of highly conductive PEMs.[33,34]

The presently available state-of-the-art membrane materials for PEM fuel cells are perfluorinated sulfonic acid (PFSA) functionalized polymers such as DuPont's Nafion and W. L. Gore's Gore-Select. The current understanding of the properties and function of these and other PEMs gleaned from experimental studies has recently been reviewed by several authors.[35−41] These electrolytes are two-phase systems, containing water dispersed as a second phase in a principally amorphous polymeric (e.g. fluorocarbon, aromatic) primary phase.[42,43] The water solvates the polymeric acidic groups and promotes proton mobility via both structural diffusion[44,45] (i.e. Grotthuss-type "hopping" of the protons through the hydrogen-bonded network of water molecules) and vehicular motion (i.e. coupled proton-water transport of hydronium ions).[46] In both transport mechanisms, the presence of water is critical in the formation of hydrated protons (i.e. as Zundel, $H_5O_2^+$, or Eigen, $H_9O_4^+$, cations) and mobility of the protons. The hydration requirement of conventional PEMs results in a problematic operating temperature limited to the boiling point of water (i.e. $T \leq 100$°C at 1 atm).

Several different approaches have been used in attempts to improve proton conduction in PEMs.[36,47] These include the use of alternative fluids (e.g. phosphoric acid and polybenzimidazole,[48,49] phosphonic acid,[50] and imidazole[51,52]) to replace the function of water in the membrane, the addition of inorganic particles[37] (e.g. silica, heteropolyacids) into polymeric conductors that purportedly allow proton conduction along the inorganic surface or maintain the water content of the membrane by adding an additional hydrophilic component, and, as alluded to above, the preparation of various alternative proton-conducting polymers. Along with the synthesis and testing of entirely novel PEMs has come modification of specific molecular features of presently available PFSAs, including the use of alternate protogenic groups (e.g. phosphonic acid) and distinct backbone and/or side chain chemistry. With respect to the latter, Yang and Rajendran[53] at DuPont reported the synthesis and fuel cell testing of a PEM similar to Nafion but with a partially fluorinated backbone and a di(tetrafluoroethylene) ether sulfonic acid side chain (i.e. $CF_2CF_2OCF_2CF_2SO_3H$) that, at certain equivalent weights (EWs), gave higher proton conductivity than Nafion. The Fuel Cell Components group at 3M also recently reported the synthesis and characterization of a PFSA membrane possessing superior conductivity with the same PTFE backbone as Nafion but with the shorter $OCF_2CF_2CF_2CF_2SO_3H$ side chain.[54] An explanation, beyond simply EW differences, as to why a decrease in the length of the side chain improves the proton conductivity, remains unclear.

Differences in the proton conductivity in membranes with similar PTFE backbone but distinct side chain length were observed much earlier by the characterization and testing of the short-side-chain (SSC) PFSA (i.e. a PTFE backbone with $OCF_2CF_2SO_3H$ side chains)[55−58] first synthesized by Dow Chemical nearly two decades ago.[59] Although this PEM has a similar morphology to Nafion as determined by SAXS and SANS experiments,[56−58] significantly higher proton conductivity than Nafion at low to intermediate water contents,[60−62] and a current density as much as three times greater than Nafion at 0.5 V in an operating fuel cell,[63] it did not see widespread application in fuel cells or even further characterization due to the substantially more difficult synthesis route as developed by Dow.[59] Recently, however, Solexis has developed a much simpler (almost a single step for both the fluorination and fluoroolefin addition) route for the synthesis of the same PEM and have reported similar superior performance when compared to Nafion.[64] As discussed earlier, the improved conductance in this SSC PFSA is not currently understood, certainly not on a molecular basis, and is therefore the provocation for the present theoretical investigation.

The present understanding of proton conduction in PEMs gleaned from theoretical investigations was recently reviewed by Paddison,[34,65] and most recently by Kreuer, Paddison et al.[3] These reviews attest to the fact that although several groups have been active in membrane modeling,[66−79] much remains to be understood in terms of the connection of properties related to fuel cell operation with molecular chemistry and hydrated morphology. A simple microstructural model, based on paramerization of a primitive cubic lattice model, has been presented by Kreuer[46] and provides a self-consistent picture of the fully hydrated membrane morphologies of Nafion and PEEKK (sulfonated polyetheretherketoneketone) as determined from SAXS (small-angle X-ray scattering) measurements over a range of hydration conditions, and water and proton self-diffusion coefficients obtained from pulsed-field gradient NMR experiments. Although this is clearly a simplistic picture, it does suggest that the chemistry of the backbone (manifesting itself in differences in rigidity and hence channel diameter), distribution (i.e. spacing) of the protogenic groups, and distinctions in acidity of these groups result in different morphological features when these materials are hydrated. A recent theoretical investigation by Khalatur et al.[80] implementing a hybrid Monte Carlo/reference interaction site model (MC/RISM) technique to probe the morphology of Nafion over a range of hydration levels showed that a continuous network of channels may exist even at very low water contents.

Extensive molecular-level modeling[13,89−99] of the acidic functional groups, polymer fragments, proton diffusion, and dielectric saturation in membrane pores for several different PEMs indicate that the proton conduction mechanism(s) in hydrated PEMs may be understood from a consideration of dissociation of the proton from the acidic site, subsequent transfer of the proton to the aqueous medium, screening by water of the hydrated proton from the conjugate base (e.g. the sulfonate anion), and finally diffusion of the proton in the confined water within the polymer matrix. High frequency (i.e. up to 30 GHz) dielectric spectroscopy[100,101] and modeling of the dielectric saturation of the water in PEMs[98,99] reveal that the confinement of the water in nanodimensioned domains with a strong electrostatic field due to dissociated sulfonic acid groups (i.e. SO_3^-) results in a lower water permittivity than in bulk water (i.e. water molecules are more tightly bound to each other and the sulfonate groups).

Ab initio electronic structure calculations of polymeric fragments with water and quantum molecular dynamics studies on model PEM systems have provided a basis for understanding the molecular ingredients in the conduction process.[34,81−89] Specifically, it was determined that (a) the dissociated state is adopted as a result of the excess positive charge being stabilized in the hydrogen bonding network of the water molecules, and the excess electron density (due to the breaking of the SO_3-H bond) sufficiently delocalized by the neighboring chemical group (anchimeric assistance), (b) the neighboring chemical group to the sulfonic acid will also impact the preferred separation of the hydronium ion after completion of the first hydration shell,

(c) hydrogen bonding between the sulfonic acid groups is favored, and, even with minimal water in the membrane, there is likely to be a continuous network of water formed among the SO_3H groups, (d) partial dissociation of the protons in a PEM will occur at water contents of less than 3 H_2Os/SO_3H, and (e) the Zundel ion ($H_5O_2^+$), as it does in bulk water, features importantly in the transfer of protons in PEMs of minimal hydration. This latter result is primarily due extensive AIMD simulations[13,34] of trifluoromethanesulfonic acid monohydrate solid (a model system for minimally hydrated perfluorosulfonic acid PEMs) where a suspected important defect structure was elucidated that possessed the distinctive features of two delocalized protons: one "shared" between two sulfonate groups and the other shared between two water molecules (i.e. a Zundel ion). With a formation free energy of only 30 kJ/mol this result suggests that a possible path to developing minimally hydrated PEMs with high proton conductivity may be through the mobility of the acidic functional groups.

Thus, with the imminent need to understand the mechanism of proton conduction in minimally hydrated PEMs, the focus of this work is on the molecular features in the SSC PFSA membrane of (i) hydration of the sulfonic acid groups, (ii) the hydrogen bonding network of the first hydration water connecting neighboring pendant side chains (i.e. sequential on the same backbone), and (iii) the role of the side chain in facilitating proton dissociation. This understanding is pursued through first principles based electronic structure calculations on fragments of the SSC ionomer consisting of two pendant side chains with different degrees of separation. Specifically, we seek to identify structures of the polymeric fragments: $CF_3CF(O(CF_2)_2SO_3H)$-$(CF_2)_nCF(O(CF_2)_2SO_3H)CF_3$, where $n = 5$, 7, and 9 both in the dry state and with from 1 to 7 explicit water molecules.

Computational Methods

All ab initio self-consistent field (SCF) molecular orbital calculations were performed using the GAUSSIAN 03 suite of programs[102] on Linux/MPI Beowulf clusters consisting of Intel Itanium 2 1.3 and 1.5 GHz dual and quad processor nodes. Starting geometries for all of the two side chain fragments were constructed by adding two side chains (i.e. 2 × [OCF_2CF_2-SO_3H]) to previously optimized (HF/6-31G**) perfluoroalkane backbone units (namely C_9F_{20}, $C_{11}F_{24}$, $C_{13}F_{28}$), the latter always exhibiting fully extended geometries (i.e. the carbon atoms in an anti arrangement and the fluorine atoms staggered when viewed down the length of the chain). Full optimizations were undertaken by conjugate gradient methods[103] without symmetry constraints using Hartree−Fock theory with the 6-31G(d,p) split valence basis set[104] from typically four different initial structures with the PTFE backbone and the side chains in various configurations and orientations. The resulting equilibrium structures were then further refined using density functional theory with Becke's three-parameter functional (B3LYP),[105−107] initially with the same 6-31G(d,p) basis set and finally with the slightly larger 6-311G**.[108] The effects of diffuse functions on the minimum energy structures were assessed and only minor differences in the structural parameters accompanied with a systematic difference in the total electronic energy was observed. Water molecules were then sequentially added to the B3LYP/6-311G(d,p) minimum energy structures to assess (i) hydrogen bond formation with the terminal sulfonic acid groups and (ii) the onset of proton dissociation. Initial structures were again, typically prepared by placing the water molecule(s) in four different positions around the sulfonic acid group(s). Vibrational frequencies and zero point energies were determined for all global minimum energy structures at the B3LYP/6-311G(d,p) level. Binding energies of the water molecules to the oligomeric fragments were calculated from both the uncorrected and ZPE corrected total electronic energies. Finally, the effect of basis set superposition error (BSSE) on the water binding energies where explored using the commonly employed counterpoise (CP) method of Boys and Bernardi.[109,110] Although BSSE corrections have been known to change the order of local minima from that predicted by uncorrected energies,[111−113] it was not anticipated that this would be the case for these fragments due to the strong binding of the water to the sulfonic acid groups. Nevertheless, binding energies were computed from CP-corrected geometry optimizations[114,115] for all hydrated fragments, which we remark was an extremely computationally expensive process, particularly for the larger fragments with seven explicit water molecules (i.e. the structure on the CP-corrected potential energy surface typically requiring more than 600 CPU hours on a 4 processor Itanium 2 node when started from the B3LYP/6-311G** minimum energy structure).

Results and Discussion

'Dry' Fragments. As described in Computational Methods, two (distinct) side chain fragments ($OCF_2CF_2SO_3H$) were attached to PTFE chains containing 9, 11, and 13 carbons that exhibited fully extended geometries (optimized at the HF/6-31G** level) and new equilibrium conformations sought, initially at the HF/6-31G** level. The presence of the side chains had little effect on the backbone conformation: the carbon atoms remained in an anti conformation even after full optimization with the hybrid density functional method and 6-311G** basis set was performed. The B3LYP/6-311G** minimum energy structures of the 'dry' oligomeric fragments with differing side chain separation are displayed in Figures 1a−c. The following nomenclature is hereafter used to refer to the fragments, denoting the number of carbon atoms between the two side chains excluding the carbon joining the first side chain to the backbone but including that joining the second: C6 (shown in Figure 1(a)), C8 (shown in Figure 1b) and C10 (shown in Figure 1c). Although many searches were undertaken from as many as three different starting geometries, including those where the terminal sulfonic acid groups were brought close enough to hydrogen bond with one another, the side chains always remained well separated in the minimum energy conformations. These results are in contrast to results presented earlier by one of the authors, where for the $CF_3CF(O(CF_2)_2SO_3H)(CF_2)_4CF(O(CF_2)_2SO_3H)$-$CF_3$ fragment (i.e. C5 using the current nomenclature) the global minimum was obtained with the sulfonic acid groups doubly hydrogen-bonded to one another.[34] Evidently, separating the terminal sulfonic acid groups by more than two tetrafluoroethylene units precludes the hydrogen bonding of the sulfonic acids with these short side chains when the backbone is fully extended. Figure 2 displays minimum energy conformations for the same three fragments but with the side chains on opposite sides of the backbone (i.e. trans relative to one another). The total electronic energy, and the (unscaled) zero point energy, are reported in Tables 1−3, and comparison of the energies for these fragments with the energies of those equilibrium structures displayed in Figure 1 shows that the cis conformations are stabilized by 4.0 and 2.2 kcal/mol for the C6 and C8 fragments, respectively. The source of this stabilization is probably a long-range interaction of the sulfonic acid groups that is absent in the trans conformations and decreases as the separation of the groups is increased. In fact, in the fragment with the greatest side chain separation (i.e. C10), the trans conformation (see

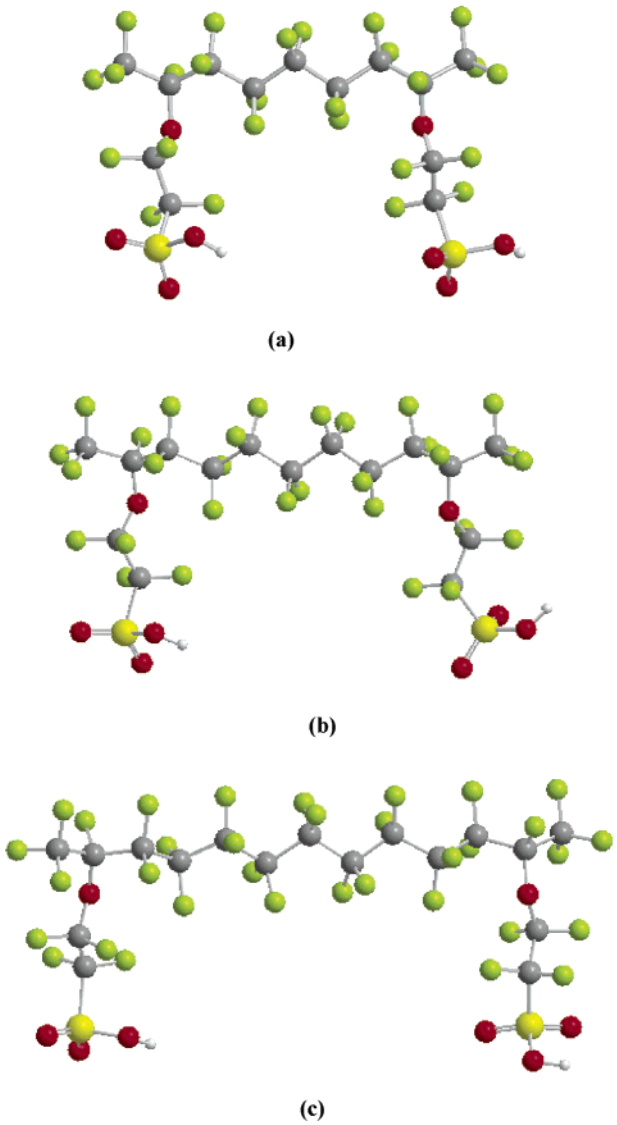

Figure 1. Fully optimized (B3LYP/6-311G**) global minimum energy structures of isolated two side chain fragments of the short-side chain perfluorosulfonic acid polymer showing the side chains on the same 'side' of the backbone: (a) the C6 fragment with three tetrafluoroethylene backbone units in the repeat monomer unit; (b) the C8 fragment with four tetrafluoroethylene backbone units in the repeat monomer unit; (c) the C10 fragment with five tetrafluoroethylene backbone units in the repeat monomer unit. Grey spheres are carbon atoms. Lime green spheres are fluorine atoms. Red spheres are oxygen atoms. Yellow spheres are sulfur atoms. White spheres are hydrogen atoms.

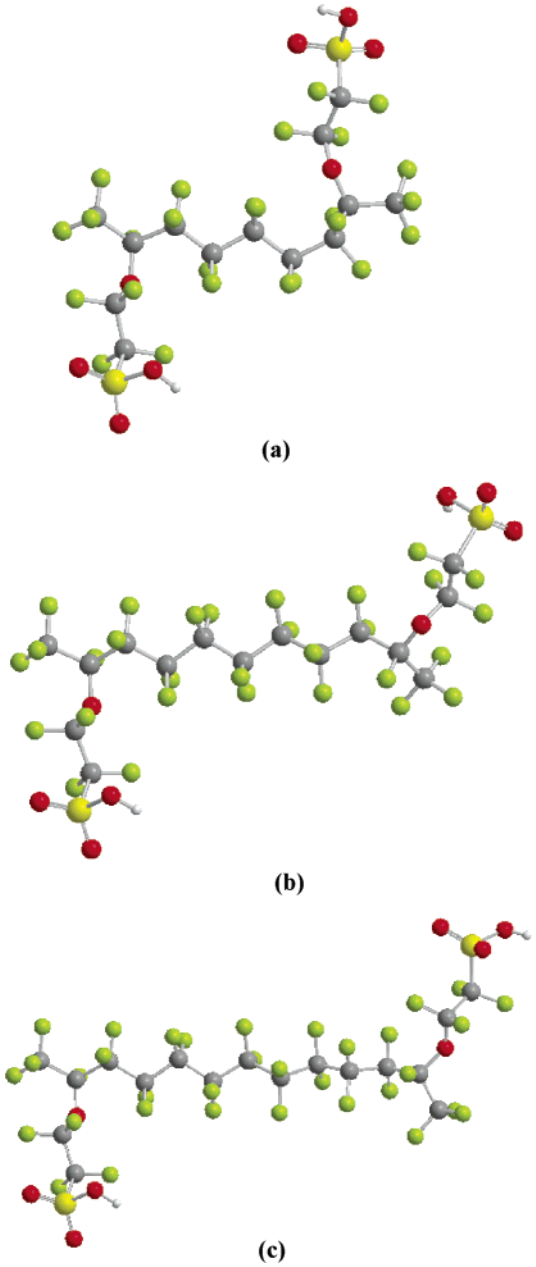

Figure 2. Fully optimized (B3LYP/6-311G**) global minimum energy structures of isolated two side chain fragments of the short-side chain perfluorosulfonic acid polymer showing the side chains anti relative to one another along the backbone: (a) the C6 fragment; (b) the C8 fragment; (c) the C10 fragment.

Figure 2c) has a zero-point corrected energy that is 1.2 kcal/mol *lower* than the cis conformation, confirming that any interaction of the sulfonic acid groups is lost when the side chains are extensively separated. It is important to realize, however, that although optimizations were begun from as many as five different starting geometries, it is quite possible that conformations of the fragments with lower energy and/or slightly distinct geometries may exist and this could result in a difference in the favorability of the cis over the trans conformations, or vice versa. Clearly, these results do not preclude the presence of both cis and trans conformations in the dry state of an actual macromolecule of the polymer. As a means of assessing changes to the oligomeric fragments upon hydration, the structural parameters for the B3LYP/6-311G** global minimum energy conformations are collected together in Tables 4, 5, and 6. Examination of selected parameters for these 'dry' fragments shows that the separation distance of the tertiary carbons on the backbone (second column of Tables 4−6) is essentially unchanged with the alteration of the orientation of the side chains (i.e. cis to trans) and scales with the number of fluoromethylene groups separating the chains, as expected. It is also worth noting that the distance separating the sulfur atoms in the sulfonic acid groups for the cis conformations differs by no more than approximately 1 Å from the separation of the respective tertiary carbons in the specific fragment.

Water 'Connected' Fragments. As one of the goals of the present work is to understand molecular connectivity of sequential sulfonic acid groups along the backbone in PEMs, water molecules were explicitly added to each of the structures in Figure 1 and full optimizations performed from a variety of different initial positions of the water molecule(s). In all cases, it was found that the resulting conformations possessing the

TABLE 1: Energies of Optimized $CF_3CF(O(CF_2)_2SO_3H)(CF_2)_5CF(O(CF_2)_2SO_3H)CF_3$ Fragments[a]

+ *n* H_2O	E_{elec}[b]	E_{ZPE}[c]	ΔE[d](kcal/mol)	ΔE_{ZPE}[e](kcal/mol)	ΔE_{BSSE}[f](kcal/mol)
0	−4491.47776193	0.213606			
trans	−4491.47146786	0.213725			
1	−4567.95856261	0.239267	−20.9	−18.2	−16.2
4	−4797.36111397	0.310524	−58.7 (−14.7)[g]	−51.4 (−12.8)†	−43.1 (−10.8)†
5	−4873.84106731	0.338394	−79.1 (−15.8)	−67.7 (−13.5)	−60.0 (−12.0)
6	−4950.34674691	0.367645	−115.6 (−19.3)	−99.2 (−16.5)	−88.6 (−14.8)
7	−5026.82049318	0.392938	−132.1 (−18.9)	−113.2 (−16.2)	−103.0 (−14.7)

[a] For structures optimized at the B3LYP/6-311G** level. [b] Total electronic energy in Hartrees. [c] Zero point energy (ZPE) in Hartrees. [d] Binding energy based on (uncorrected) total electronic energies. [e] Binding energy based on ZPE corrected E_{elec}. [f] Binding energy based on CP correction to BSSE of reoptimized structure. [g] Values in parentheses are per water molecule.

TABLE 2: Energies of Optimized $CF_3CF(O(CF_2)_2SO_3H)(CF_2)_7CF(O(CF_2)_2SO_3H)CF_3$ Fragments[a]

+ *n* H_2O	E_{elec}[b]	E_{ZPE}[c]	ΔE[d] (kcal/mol)	ΔE_{ZPE}[e] (kcal/mol)	ΔE_{BSSE}[f] (kcal/mol)
0	−4967.17008609	0.237984			
trans	−4967.16634648	0.237742			
2	−5120.1173770	0.288006	−32.9 (−16.4)[g]	−28.2 (−14.1)†	−25.1 (−12.6)†
3	−5196.59332136	0.312857	−50.8 (−16.9)	−43.9 (−14.6)	−39.1 (−13.0)
4	−5273.0514513	0.336390	−57.5 (−14.4)	−49.2 (−12.3)	−42.6 (−10.6)
5	−5349.55024136	0.363704	−89.7 (−17.9)	−77.7 (−15.5)	−65.3 (−13.1)
6	−5426.01195092	0.389560	−98.6 (−16.4)	−83.8 (−14.0)	−77.5 (−12.9)
7	−5502.48748578	0.413843	−116.2 (−16.6)	−99.5 (−14.2)	−88.5 (−12.6)

[a] For structures optimized at the B3LYP/6-311G** level. [b] Total electronic energy in Hartrees. [c] Zero point energy (ZPE) in Hartrees. [d] Binding energy based on (uncorrected) total electronic energies. [e] Binding energy based on ZPE corrected E_{elec}. [f] Binding energy based on CP correction to BSSE of reoptimized structure. [g] Values in parentheses are per water molecule.

TABLE 3: Energies of Optimized $CF_3CF(O(CF_2)_2SO_3H)(CF_2)_9CF(O(CF_2)_2SO_3H)CF_3$ Fragments[a]

+ *n* H_2O	E_{elec}[b]	E_{ZPE}[c]	ΔE[d] (kcal/mol)	ΔE_{ZPE}[e] (kcal/mol)	ΔE_{BSSE}[f] (kcal/mol)
0	−5442.86698579	0.261831			
trans	−5442.86902479	0.261939			
3	−5672.28318483	0.336627	−46.3 (−15.4)[g]	−39.5 (−13.2)†	−34.0 (−11.3)†
4	−5748.75896901	0.361436	−64.1 (−16.0)	−55.1 (−13.8)	−47.9 (−12.0)
5	−5825.21666004	0.384827	−70.6 (−14.1)	−60.2 (−12.0)	−51.5 (−10.3)
6	−5901.71043316	0.413976	−99.6 (−16.6)	−84.4 (−14.1)	−75.8 (−12.6)
7	−5978.18669335	0.441087	−117.7 (−16.8)	−98.8 (−14.1)	−87.7 (−12.5)

[a] For structures optimized at the B3LYP/6-311G** level. [b] Total electronic energy in Hartrees. [c] Zero point energy (ZPE) in Hartrees. [d] Binding energy based on (uncorrected) total electronic energies. [e] Binding energy based on ZPE corrected E_{elec}. [f] Binding energy based on CP correction to BSSE of reoptimized structure. [g] Values in parentheses are per water molecule.

TABLE 4: Structural Data[a] from Optimized[b] $CF_3CF(O(CF_2)_2SO_3H)(CF_2)_5CF(O(CF_2)_2SO_3H)CF_3$ Fragments

+ *n* H_2O	CF···CF	S···S	SO_2O···H	O···O	Figure no.
0	7.89	9.03	0.97		1a
trans	7.82	13.8	0.97		2a
1	7.87	7.18	1.02, 0.97	2.56, 2.91	3a
4	7.86	7.51	1.10, 1.02	2.44, 2.60, 2.89	4a
5	7.86	6.97	1.41, 1.47	2.49, 2.51	4b
6	7.84	6.53	1.67, 1.54	2.64, 2.56,	4c
7	7.83	6.29	1.67, 1.58	2.64, 2.58	4d

[a] All bond distances in angstoms. [b] Optimized at the B3LYP/6-311G** level.

TABLE 5: Structural Data[a] from Optimized[b] $CF_3CF(O(CF_2)_2SO_3H)(CF_2)_7CF(O(CF_2)_2SO_3H)CF_3$ Fragments

+ *n* H_2O	-CF···CF-	-S···S-	SO_2O···H	O···O	Figure no.
0	10.50	11.44	0.97		1b
trans	10.53	16.58	0.97		2b
2	10.49	9.37	1.04, 0.97	2.51, 2.70, 2.94	3b
3	10.49	9.33	1.04, 1.02	2.51, 2.70, 2.91	5a
4	10.49	9.18	1.06, 1.02	2.48, 2.67, 2.90	5b
5	10.45	8.95	1.65, 1.02	2.64, 2.47, 2.90	5c
6	10.49	10.2	3.04, 1.02	2.66, 2.43, 2.71, 2.94	6a
7	10.47	9.45	1.59, 1.37	2.58, 2.46, 2.66, 2.85	6b

[a] All bond distances in angstoms. [b] Optimized at the B3LYP/6-311G** level.

lowest energies were ones where the water molecules are hydrogen-bonded to both sulfonic acid groups, with the caveat that there must be a sufficient number of water molecules in the cases where the side chains are well separated. Fully optimized (at the B3LYP/6-31G**) geometries where initially determined for polymeric fragments without a sufficient number of water molecules to connect the sulfonic acid groups (i.e. for the C8 + 1 H_2O and the C10 + 2 H_2O); but as these structures only exhibited conformations with a water molecule hydrogen bonded to either (C8 + 1 H_2O) or both (C10 + 2 H_2O) sulfonic acid group(s) similar to previously reported water clusters of single side chain fragments of this same polymer,[34] we do not include these results (either structures or energies) in the present work. The resulting B3LYP/6-311G** global minimum energy structures for all three oligomeric fragments are displayed in Figure 3a−c and collectively show that the number of water molecules required to connect or bridge the terminal groups is proportional to the number of difluoromethylene groups in the backbone: one water molecule for five CF_2 groups (C6), two water molecules for seven CF_2 groups (C8), and three water molecules for nine CF_2 groups (C10). All structures show that the hydrogen bonding through the water is from the acidic proton from one of the sulfonic acid groups to an oxygen atom of the adjacent sulfonic acid. Thus, the connectivity of the acidic protons is via a network or 'wire' of hydrogen bonds through both acidic groups and the water molecule(s). The B3LYP/6-311G** binding energies (uncorrected, ZPE corrected, and

TABLE 6: Structural Data[a] from Optimized[b] $CF_3CF(O(CF_2)_2SO_3H)(CF_2)_9CF(O(CF_2)_2SO_3H)CF_3$ Fragments

+ *n* H_2O	-CF···CF-	-S···S-	$-SO_2O\cdots H$	O···O	Figure no.
0	13.10	13.52	0.97		1c
trans	13.13	18.2	0.97		2c
3	13.07	11.48	1.06, 0.97	2.49, 2.65, 2.76, 2.98	3c
4	13.07	11.47	1.06, 1.02	2.48, 2.64, 2.75, 2.94	7c
5	13.08	11.37	1.09, 1.02	2.45, 2.62, 2.74, 2.93	7c
6	12.99	9.70	1.63, 1.02	2.60, 2.46, 2.71, 2.98	7c
7	13.01	9.60	1.65, 1.01	2.62, 2.47, 2.66, 3.01	7c

[a] All bond distances in angstoms. [b] Optimized at the B3LYP/6-311G** level.

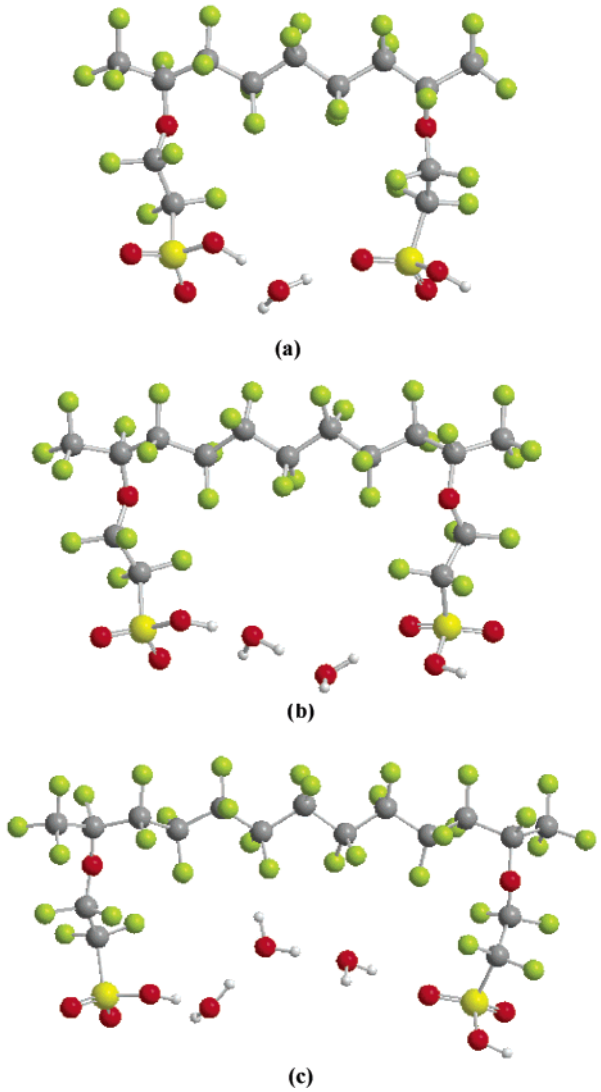

Figure 3. Fully optimized (B3LYP/6-311G**) global minimum energy structures of two side chain fragments of the short-side chain perfluorosulfonic acid polymer showing the connectivity of the hydrophilic groups with explicit water molecules: (a) one H_2O connects the sulfonic acid groups in the C6 fragment; (b) two H_2Os connect the sulfonic acid groups in the C8 fragment; (c) three H_2Os connect the sulfonic acid groups in the C10 fragment.

BSSE corrected) of the water molecule(s) to the sulfonic acids for the oligomeric fragments in Figure 3a−c are reported in the third row of Tables 1−3. Comparison of the different methods of computing the binding energy reveals that the absolute magnitude of the binding energy per water molecule is uniformly reduced by more than 2 kcal/mol when corrected for zero-point energy and by approximately 4 kcal/mol when corrected for basis set superposition error for optimized structures on CP-corrected potential energy surfaces. The latter clearly suggests the importance of correcting for BSSE if one is to obtain an absolute measure of the interaction of the 'chemical' or first hydration shell water molecule(s) to these strong Brønsted−Lowry acids. However, the relative trend between the three oligomeric fragments remains the same across the three methods employed in the calculation of the binding energy. Specifically, the magnitude of the binding energy decreases (per water molecule) as the side chains are separated with energies corrected for BSSE with values of: 16.2, 12.6, and 11.3 kcal/mol for the C6, C8, and C10 fragments, respectively.

The structural data in Tables 4−6 show that the oxygen−hydrogen bond distance of the acidic proton involved in the hydrogen bond network has slightly lengthened over that in the isolated oligomeric fragments, i.e., 0.97 Å, and that the hydrogen bond distance (as measured by the oxygen−oxygen distance) is uniformly the shortest among the three different oligomeric fragments, at only about 2.5 Å with the acidic proton, and then becomes progressively longer along the network to a length of more than 2.9 Å at the oxygen of the other sulfonic acid group. This difference in hydrogen bond length is due to the first water molecule acting as a nucleophile to the highly acidic proton, and the last water molecule along the chain as an electrophile. Although this set of conformations suggests a plausible transfer path for the protons between the sulfonic acid groups through the 'nearest' (to the sulfonic acids) neighbor water molecules, it is important to realize that the transfer of a proton to a sulfonate group is not barrierless. As expected with strong Brønsted−Lowry acids: the proton is readily donated but not accepted. The collected data in Tables 4−6 also show that while the distance between the carbons where the side chains are tethered to the backbone has changed very little from the dry oligomeric fragments, the distance between the terminal groups has been consistently contracted through formation of the water network by approximately 2 Å. This suggests that some flexibility or lability in the side chains is observed through the hydrogen bonding of only a very small amount water with the sulfonic acid groups. Hence, these calculations do reveal the possible cooperative role of the side chains in facilitating proton transfer in minimally hydrated PFSAs. Finally, it is worth noting that in connecting the sulfonic acid groups with a minimal 'wire' of water molecules, little change has been observed in the backbone geometry for any of these oligomeric fragments.

Proton Dissociation. Previous work with single (i.e. isolated) perfluorosulfonic acid molecules indicated that dissociation was not observed until three water molecules were added to the acid molecule.[82,86] It was reasoned that to effect dissociation there must be sufficient water molecules to stabilize the excess negative charge on the oxygen atoms of the sulfonate conjugate base. Thus, to understand the influence of the proximity of a second sulfonic acid group on the transfer of the proton(s) to the water molecules in the first hydration shell, additional water molecules were systematically added to the fragments shown in Figure 3. The same protocol as was previously employed (i.e. an initial HF/6-31G** optimization followed by B3LYP/6-31G** and finally B3LYP/6-311G** optimizations) was implemented to obtain minimum energy conformations for all of the two side chain fragments with local hydration of 4, 5, 6, and 7 water molecules. The resulting structures and energies for each fragment are discussed in the following subsections separately.

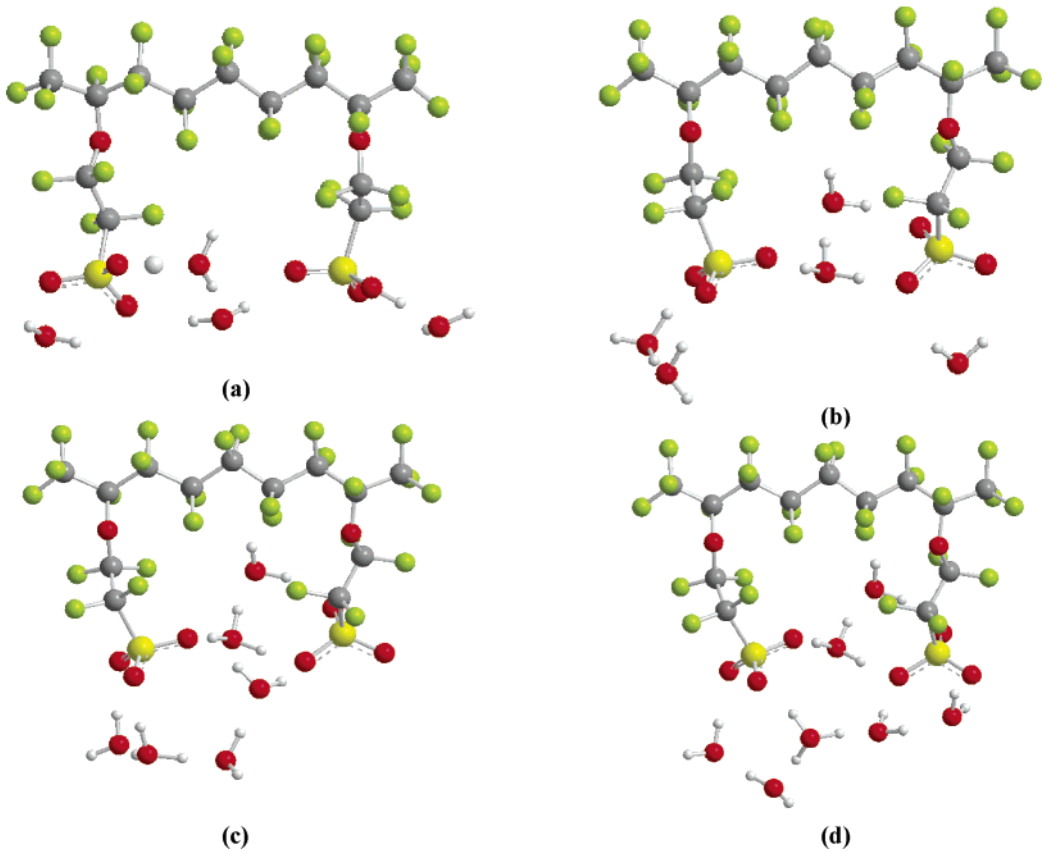

Figure 4. Fully optimized (B3LYP/6-311G**) global minimum energy structures of the C6 two side chain fragment showing hydration and proton dissociation as additional water molecules are added: (a) no dissociation of either acidic proton with four H_2Os, although the O−H bond distance in one of the sulfonic acid groups is lengthened 1.10 Å; (b) both protons dissociation with the hydration of five H_2Os; (c and d) the hydrated protons in Zundel-ion-like configurations that further separate with hydration of six and seven H_2Os, respectively.

C6 Fragment + 4−7 H_2Os. The B3LYP/6-311G** fully optimized structures for the C6 fragment with nine carbon atoms in the backbone are displayed in Figure 4a−d, with the energies and selected structural data reported in Tables 1 and 4, respectively. Examination of the calculated binding energies reveals that the trend in the binding energy calculated per water molecule is consistent among the three methods. Specifically, the binding energy per water molecule decreased from that with only a single water molecule (Figure 3a) as the water molecules were added, until proton dissociation occurred. With proton dissociation, and subsequent separation of the hydronium ions from the sulfonate groups, the magnitude of the binding energy increased to a value of 14.7 kcal/mol for the fragment with seven water molecules when computed on the CP-corrected potential energy surface. The lowest energy conformation of the oligomeric fragment with four added water molecules (Figure 4a) showed no proton dissociation but an increase in the oxygen−hydrogen bond distance of nearly 0.1 Å for both sulfonic acid protons and some increased separation of the terminal side chain groups (>0.3 Å). The distance (along the backbone) between the tertiary carbons remained essentially constant in the equilibrium structures as the water molecules were added, indicating little conformational change in the backbone. Of several minimum energy structures determined after five water molecules were added, the structure in Figure 4b showing dissociation of both protons possessed the lowest energy. In previous work[82,86] that examined the hydration and proton dissociation of single (i.e. isolated) sulfonic acids it was observed that three water molecules were required to observe the transfer of the proton to the water, but the current result indicates that close proximity of another sulfonic acid may reduce the number of water molecules per sulfonic acid required to stabilize the protonic charge in the first hydration shell. Of additional significance is the result that both dissociated protons appear as 'Zundel ion'-like (i.e. $H_5O_2^+$) in the global minimum conformation, with one of the hydrated protons bridging the two sulfonate groups. This result is very similar to that determined via AIMD as a stable protonic defect in the trifluoromethanesulfonic acid monohydrate solid, where in the unit cell (i.e. $[CF_3SO_3H]_4$) one proton is 'shuttled' between two sulfonate groups and another 'shuttled' between a pair of water molecules as a Zundel ion.[13] The global minimum energy structures of the same oligomeric fragment with six and seven added water molecules are shown Figure 4c and 4d and indicated that the additional water has not appreciably changed either the presence or position of the dissociated protons: they remain Zundel-like. The tabulated structural data (Table 4) indicates that the additional water molecules have resulted in a greater separation of the transferred protons from their conjugate bases and a bringing together of the sulfonate groups.

C8 Fragment + 3−7 H_2Os. Binding energies computed from both uncorrected and ZPE corrected total electronic B3LYP/6-311G** energies, along with those corrected for BSSE with optimization under the CP method, are reported for the C8 fragment in Table 2. Examination of the binding energies as the number of water molecules is increased again shows a similar trend as was observed with the smaller C6 fragment with the water molecules more tightly bound to the polymeric fragment upon dissociation of the protons. This is particularly evident when comparing the computed BSSE corrected binding energy upon dissociation of the proton (i.e. after five H_2Os were added, Figure 5c) to that immediately prior (i.e. Figure 5b with

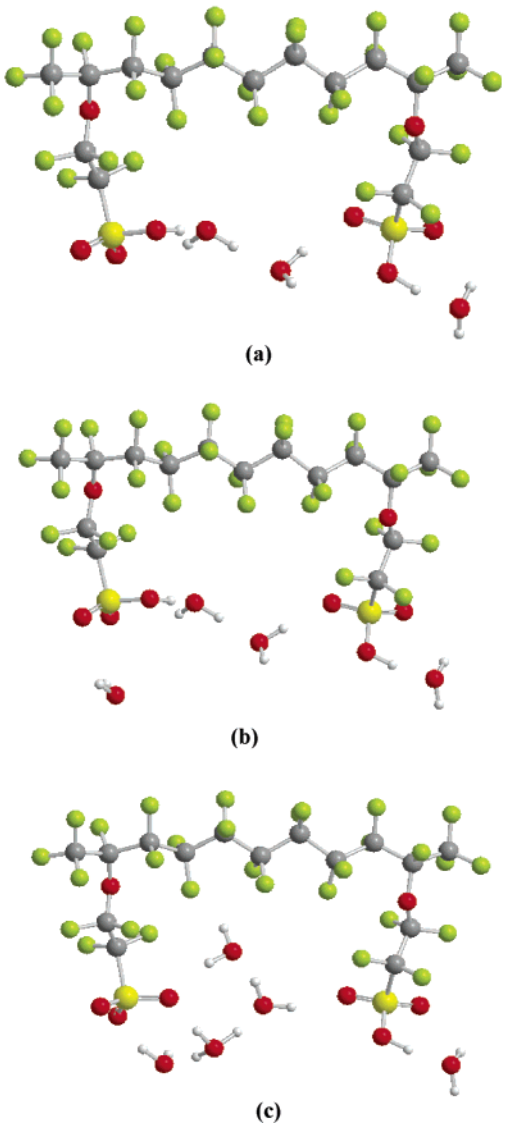

Figure 5. Fully optimized (B3LYP/6-311G**) global minimum energy structures of the C8 two side chain fragment showing hydration and proton dissociation as three additional (beyond the connected fragment in Figure 3a) water molecules are added: (a and b) no proton dissociation was witnessed with addition of either three or four H_2Os, respectively; (c) dissociation of only one of the protons occurs after five H_2Os are added.

four H_2Os): where the magnitude, per water molecule, increased by 2.5 kcal/mol. Although proton dissociation did not occur until five water molecules were added to either the C6 or C8 fragment, it is important to realize the qualitative difference between the two fragments: both protons dissociated in the fragment with one fewer tetrafluoroethylene group separating the side chains, whereas only one proton was transferred to the water molecules in the fragment with greater side chain separation (Figure 5c). This result clearly suggests that the separation of the sulfonic acid groups will affect the minimum amount of water needed to witness dissociation of the protons. Although the magnitude of the binding energy per water molecule is similar between the C6 and C8 fragments when only four water molecules were added (~10.7 kcal/mol) with the subsequent addition of three further water molecules the magnitude increased to ~13.0 kcal/mol and remained nearly unchanged. This is in contrast to the C6 fragment where significant increases in the magnitude of the water binding

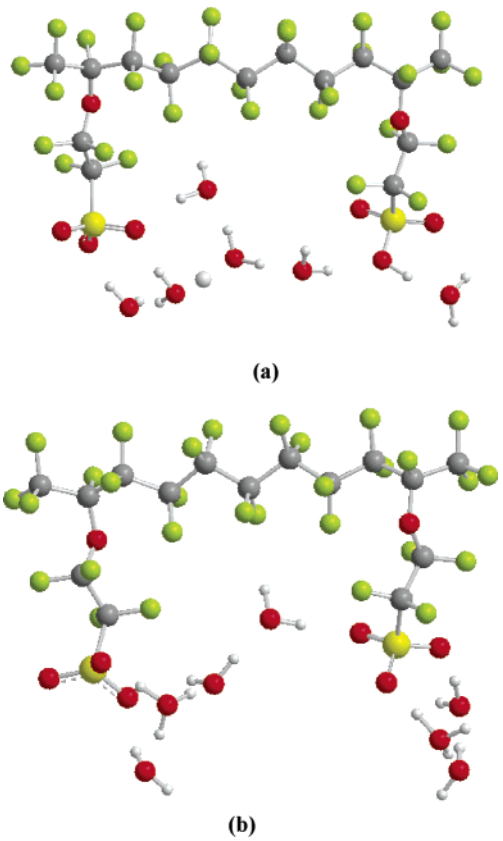

Figure 6. Fully optimized (B3LYP/6-311G**) global minimum energy structures of the C8 two side chain fragment showing hydration and proton dissociation as additional water molecules are added: (a) with a hydration consisting of six H_2Os only one of the protons has been transferred to the water molecules and exists as a 'true' Zundel ion in this minimum energy conformation; (b) finally after seven H_2Os are added dissociation of the second proton is witnessed, but this conformation shows the hydrated protons in separate water clusters.

energies were observed of nearly 3 kcal/mol with either six or seven water molecules.

The global minimum energy structures obtained at the B3LYP/6-31G** level for the C8 fragment with three, four, and five explicit water molecules are shown in Figure 5a−c and with six and seven added water molecules in Figure 6a and 6b. The selected structural parameters for this polymeric fragment as the number of added water molecules was increased are reported in Table 5. Comparison of these structures with the fragment with minimal amount of water to afford connectivity between the sulfonic acid groups (i.e. + 2 H_2O) reveals that very little change has occurred in the conformation of the PTFE portion of the fragment as the water molecules were added. The separation of the tertiary backbone carbons has remained essentially fixed at a distance of approximately 10.5 Å. In addition, the structural data reveals that only small changes occurred in the separation of the side chain termini with successive small decreases observed when four and five water molecules were added followed by an increase (of > 1 Å) when six water molecules were added. The C8 fragment with six water molecules is quite interesting in that the single dissociated proton in the global minimum energy structure (Figure 6a) has adopted a 'true' Zundel cation state with an O···O distance of 2.45 Å. This result is very similar to that reported earlier for a smaller fragment of the SSC PFSA, with the same number (i.e. six) of explicit water molecules, but only two tetrafluoroethylene backbone units separating the side chains.[13] This finding again attests to the importance of structural diffusion in the transport

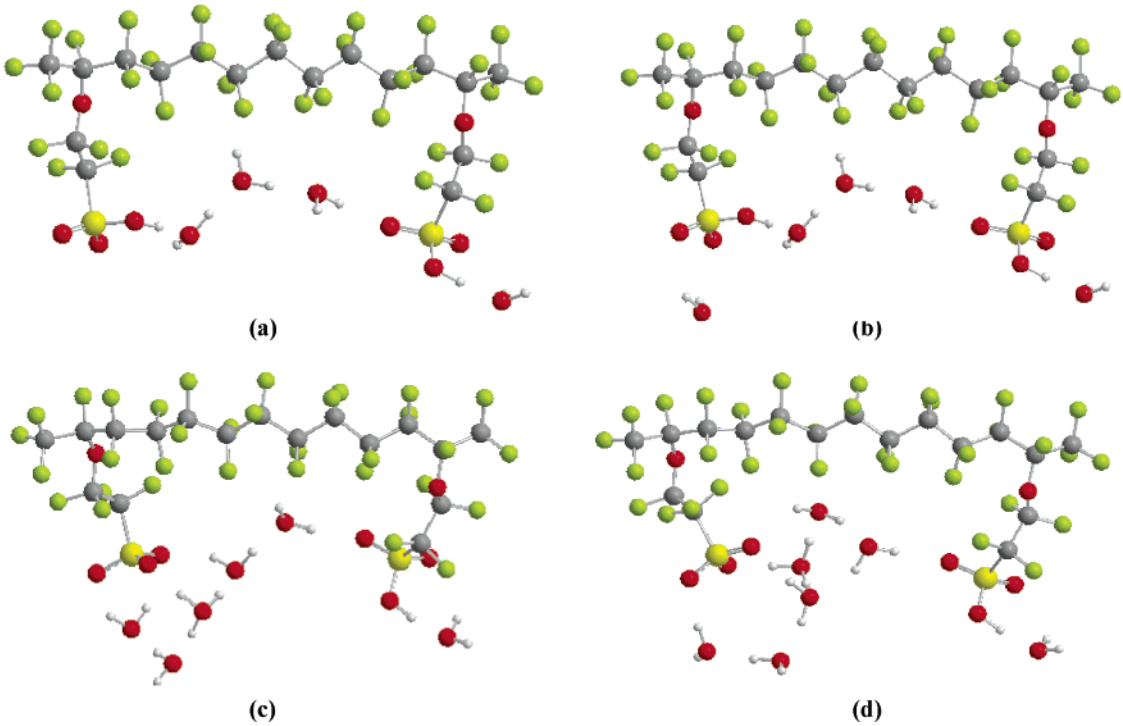

Figure 7. Fully optimized (B3LYP/6-311G**) global minimum energy structures of the C10 two side chain fragment showing hydration and proton dissociation as additional (beyond the connected fragment in Figure 3c) water molecules are added: (a and b) no protons dissociate with hydrations of four and five H_2Os, respectively; (c) dissociation of only one of the protons occurs with a hydration of six H_2Os; (d) the second proton did not dissociation after seven H_2Os were added, though the terminal sulfon-ic/ate groups moved closer to one another due to conformational changes in the side chains.

of protons even in the (immediate) proximity of negatively charged SO_3^- groups. The global minimum energy structure of this fragment with seven water molecules (Figure 6a) shows the dissociation of the second proton, but unlike the result obtained with the corresponding hydration of C6 fragment, the water molecules are separated into two groups linked only through one of the sulfonates.

C10 Fragment + 4−7 H_2Os. The fully optimized structures for the largest fragment of the SSC membrane examined in this comparative study, computed at the B3LYP/6-311G** level, are displayed in Figure 7a−d; with the energies and selected structural data reported in Tables 3 and 6, respectively. The magnitude of the total binding energy decreased, similar to that observed with both the C6 and C8 fragments, when compared across the methods according to: $|\Delta E| > |\Delta E_{ZPE}| > |\Delta E_{BSSE}|$. The binding energies also show the same trend as discussed above for the smaller fragments: the magnitude increased by more than 2 kcal/mol with the onset of proton dissociation (+ six H_2Os). Although the magnitude of the binding energies (per water molecule) with clusters of six and seven water molecules and are similar to the C8 fragment, it is important to realize that with this fragment no dissociation of the second proton was observed. This suggests that with the extent of the separation of the sulfonic acid groups afforded by this fragment, i.e., > 9.5 Å, the water does not set up as extensive a network with the hydrophilic groups. Examination of the minimum energy structure with four and five added water molecules reveals that the equilibrium conformations are very similar to the fragment with three water molecules, with little change in either the backbone or the hydrogen bond network of water molecules connecting the sulfonic acid groups. The observation of dissociation of either of the protons was not witnessed until six water molecules were added, in contrast to that observed in the lower molecular weight fragments. The transfer of one of the acidic protons to the water is accompanied by an increase in the binding energy per water molecule and, importantly, a decrease in the separation of the protogenic groups. The addition of a further water molecule did not result in an equilibrium structure with the second proton transferred. It is clear from the data in Table 6 that there is little difference in either the polymer backbone or the hydrogen bond network in this fragment with clusters of either six or seven H_2Os. The decrease in the separation of the protogenic groups after proton dissociation is the result of changes in the conformations of the side chains only: the $OCF_2CF_2SO_3$ dihedral angle in each side chain decreased by nearly 20°. These results with the larger water clusters suggest that with sufficient water some conformational change in the side chains occurs to facilitate either the hydration of the sulfonic acid groups or proton dissociation.

Conclusions

The number of difluoromethylene groups in the backbone separating the side chains in SSC PFSA membranes affects the connectivity of the terminal sulfonic acid groups. Specifically, with more than four difluoromethylene groups no hydrogen bonding occurs between neighboring sulfonic acid groups on the same backbone when no water is present. The number of water molecules required to form a continuous hydrogen-bonded network between the terminal sulfonic acid groups on the side chains is also a function of the number of difluoromethylene groups on the backbone separating the side chains. Specifically, it was found that one, two, and three water molecules bridged the sulfonic acid groups when five, seven, and nine (CF_2) separated the chains, respectively. The separation along the polymeric backbone of the side chains affects the minimum amount of water necessary to observe the transfer of proton(s) to the first hydration shell. In the SSC fragment with only five

difluoromethylene groups separating the pendant side chains (C6), dissociation of both protons occurred after only five water molecules were added whereas the fragments with seven and nine (CF_2) groups (C8 and C10) required five and six water molecules to effect dissociation of only one of the acidic protons, respectively. Even after the addition of seven water molecules, no transfer of the second proton was observed in the largest fragment (C10). All of the SSC fragments with differing separation of the side chains confirm the importance of the Zundel ion ($H_5O_2^+$) in the first hydration shell under the minimally hydrated (i.e. 3 H_2O/SO_3H) conditions examined. These calculations suggest that despite the hydrogen bonding of the water molecules with the conjugate base (i.e. SO_3^-), transfer of the protons via structural diffusion will still occur. Finally, these calculations have demonstrated that side chain separation affects the establishment of a hydrogen bond network of the sulfonic acid groups in the short side chain Dow PEM. While these calculations do not consider the interactions of sulfonic acid groups from distinct macromolecules of the polymer, they do provide new insight into the consequences of aggregation or connectivity of the proton bearing groups. This work has also provided a benchmark set of results for which the effects of distinct and mixed protogenic groups, the consequences of differing side chain lengths, and local chemical composition may be examined.

Acknowledgment. The authors gratefully acknowledge financial support from the Engineering and Physical Sciences Research Council (EPSRC) of the UK, and S.J.P. thanks the University of Alabama—Huntsville for financial support in the purchase of one of the Beowulf clusters used in this work. We also appreciated the helpful discussions of A. Rauk (University of Calgary).

References and Notes

(1) Kreuer, K. D. *ChemPhysChem* **2002**, *3*, 771.
(2) Steele, B. C. H.; Heinzel, A. *Nature* **2001**, *414*, 345.
(3) Kreuer, K. D.; Paddison, S. J.; Spohr, E.; Schuster, M. *Chem. Rev.***2004**, *104*, 4637.
(4) Colomban, P., Ed. *Proton Conductors: Solids, membranes and gels − materials and devices*; Cambridge University Press: Cambridge, 1992.
(5) Kreuer, K. D. *Chem. Mater.* **1996**, *8*, 610.
(6) Elliott, J. A.; Paddison, S. J. *Proton Conduction in Diverse Media*, a symposium at Fitzwilliam College, University of Cambridge, April 11−12, 2005. See: http://srcf.ucam.org/~jae1001/proton_meeting/.
(7) Tuckerman, M.; Laasonen, K.; Sprik, M.; Parrinello, M. *J. Chem. Phys.* **1995**, *103*, 150.
(8) Agmon, N. *Chem. Phys. Lett.* **1995**, *244*, 456.
(9) Marx, D.; Tuckerman, M. E.; Hutter, J.; Parrinello, M. *Nature* **1999**, *397*, 601.
(10) Day, T. J. F.; Schmitt, U. W.; Voth, G. A. *J. Am. Chem. Soc.* **2000**, *122*, 12027.
(11) Lapid, H.; Agmon, N.; Petersen, M. K.; Voth, G. A. *J. Chem. Phys.* **2005**, *122*, 014506.
(12) Marrone, J. A.; Tuckerman, M. E. *J. Chem. Phys.* **2002**, *117*, 4403.
(13) Eikerling, M.; Paddison, S. J.; Pratt, L. R.; Zawodzinski, T. A., Jr. *Chem. Phys. Lett.* **2003**, *368*, 108.
(14) Slade, R. C. T.; Omana, M. J. *Solid State Ionics* **1992**, *58*, 195.
(15) Rosso, L.; Tuckerman, M. E. *Solid State Ionics* **2003**, *161*, 219.
(16) Kreuer, K. D. *Annu. Rev. Mater. Res.* **2003**, *33*, 333.
(17) Dippel, T.; Kreuer, K. D.; Lassègues, J. C.; Rodriguez, D. *Solid State Ionics* **1993**, *61*, 41.
(18) Baranov, A. I.; Shuvalov, L. A.; Schagina, N. M. *JETP Lett*. **1982**, *36*, 459.
(19) DeCoursey, T. E. *Physiol. Rev.* **2003**, *83*, 475.
(20) Smondyrev, A. M.; Voth G. A. *Biophys. J.* **2002**, *83*, 1987.
(21) Wu Y. J.; Voth G. A. *Biophys. J.* **2003**, *85*, 864.
(22) Pomès, R.; Roux, B. *Biophys. J.* **2002**, *82*, 2304.
(23) DeCoursey, T. E.; Cherny, V. V. *Isr. J. Chem.* **1999**, *39*, 409.
(24) Dellago, C.; Naor, M. M.; Hummer, G. *Phys. Rev. Lett.*, **2003**, *90*, 105902.
(25) Zawodzinski, T. A.; Neeman, M.; Sillerud, L. O.; Gottesfeld, S. *J. Phys. Chem.* **1991**, *95*, 6040.
(26) Zawodzinski, T. A.; Springer, T. E.; Davey, J.; Jestel, R.; Lopez, C.; Valerio, J.; Gottesfeld, S. *J. Electrochem. Soc.* **1993** *140*, 1981.
(27) Kreuer, K. D. *Solid State Ionics* **1997**, *97*, 1.
(28) Edmondson, C. A.; Stallworth, P. E.; Chapman, M. E.; Fontanella, J. J.; Wintersgill, M. C.; Chung, S. H.; Greenbaum, S. G. *Solid State Ionics* **2000**, *135*, 419.
(29) Tang, H.; Pintauro, P. N. *J. Appl. Polym. Sci.* **2001**, *79*, 49.
(30) Kerres, J.; Ullrich, A.; Hein, M. *J. Polym. Sci.: Part A: Polym. Chem.* **2001**, *39*, 2874.
(31) Young, S. K.; Mauritz, K. A. *J. Polym. Sci.: Part B: Polym. Phys.* **2002**, *40*, 2237.
(32) Ma, Y.-L.; Wainright, J. S.; Litt, M. H.; Savinell, R. F. *J. Electrochem. Soc.* **2004**, *151*, A8.
(33) Kreuer, K. D. *Solid State Ionics* **2000**, *136−137*, 149.
(34) Paddison, S. J. *Annu. Rev. Mater. Res.* **2003**, *33*, 289.
(35) Doyle, M.; Rajendran, G. Perfluorinated membranes. In *Handbook of Fuel Cells − Fundamentals, Technology and Applications Volume 3 − Fuel Cell Technology and Applications*; Vielstich, W., Lamm, A., Gasteiger, H., Eds.; J. Wiley and Sons: Chichester, UK, 2003.
(36) Kreuer, K. D. Hydrocarbon membranes. In *Handbook of Fuel Cells − Fundamentals, Technology and Applications Volume 3 − Fuel Cell Technology and Applications*; Vielstich, W., Lamm, A., Gasteiger, H., Eds.; J. Wiley and Sons: Chichester, UK, 2003.
(37) Alberti, G.; Casciola, M. *Annu. Rev. Mater. Res.* **2003**, *33*, 129.
(38) Schuster, M. F. H.; Meyer, W. H. *Annu. Rev. Mater. Res.* **2003**, *33*, 233.
(39) Roziere, J.; Jones, D. J. *Annu. Rev. Mater. Res.* **2003**, *33*, 503.
(40) Mauritz, K. A.; Moore, R. B. *Chem. Rev.* **2004**, *104*, 4535.
(41) Hickner, M. A.; Ghassemi, H.; Kim, Y. S.; Einsla, B. R.; McGrath, J. E. *Chem. Rev.* **2004**, *104*, 4613.
(42) Gebel, G.; Lambard, J. *Macromolecules* **1997**, *30*, 7914.
(43) Gebel, G. *Polymer* **2000**, *41*, 5829.
(44) Eigen, M.; De Maeyer, L. *Proc. R. Soc. (London), Ser. A* **1958**, *247*, 505.
(45) Eigen, M. *Angew. Chem.* **1963**, *75*, 489.
(46) Kreuer, K. D. *J. Membr. Sci.* **2001**, *185*, 29.
(47) Kerres, J. A. *J. Membr. Sci.* **2001**, *185*, 3.
(48) Wainright, J. S.; Wang, J. T.; Weng, D.; Savinell, R. F.; Litt, M. *J. Electrochem. Soc*. **1995**, *142*, L121.
(49) Glipa, X.; Bonnet, B.; Mula, B.; Jones, D. J.; Rozière, J. *J. Mater. Chem*. **1999** *9*, 3045.
(50) Allcock, HR.; Hofmann, M. A.; Ambler, C. M.; Lvov, S. N.; Zhou, X. Y. Y.; Chalkova, E.; Weston, J. *J. Membr. Sci.* **2002**, *201*, 47.
(51) Kreuer, K. D.; Fuchs, A.; Ise, M.; Spaeth, M.; Maier, J. *Electrochim. Acta* **1998**, *43*, 1281.
(52) Bozkurt, A.; Meyer, W. H.; Wegner, G. *J. Power Sources* **2003**, *123*, 126.
(53) Yang, Z. Y.; Rajendran, R. G. *Angew. Chem., Int. Ed.* **2005**, *44*, 564.
(54) Hamrock, S. Presented at Advances in Materials for Proton Exchange Membrane Fuel Cell Systems 2005, Pacific Grove, CA Feb 20−23, 2005.
(55) Tant, M. R.; Darst, K. P.; Lee, K. D.; Martin, C. W. In *Multiphase Polymers: Blends and Ionomers*; Utracki, L. A., Weiss, R. A., Eds.; ACS Proceedings Series 395, American Chemical Society: Washington, D. C., 1989; pp 370−400.
(56) Moore, R. B.; Martin, C. R. *Macromolecules* **1989**, *22*, 3594.
(57) Halim, J.; Büchi, F. N.; Hass, O.; Stamm, M.; Scherer, G. G. *Electrochim. Acta* **1994**, *39*, 1303.
(58) Gebel, G.; Moore, R. B. *Macromolecules* **2000**, *33*, 4850.
(59) Ezzell, B. R.; Carl, W. P.; Mod, W. A., Inventors; The Dow Chemical Company, Assignee. U. S. patent 4,358,412, 1982.
(60) Zawodzinski, T. A.; Springer, T. E.; Davey, J.; Jestel, R.; Lopez, C.; Valerio, J.; Gottesfeld, S. *J. Electrochem. Soc.* **1993** *140*, 1981.
(61) Edmondson, C. A.; Stallworth, P. E.; Chapman, M. E.; Fontanella, J. J.; Wintersgill, M. C.; Chung, S. H.; Greenbaum, S. G. *Solid State Ionics* **2000**, *135*, 419.
(62) Edmondson, C. A.; Fontanella, J. J. *Solid State Ionics* **2002**, *152−153*, 355.
(63) Prater, K. *J. Power Sources* **1990**, *29*, 239.
(64) Arcella, V.; Ghielmi, A.; Tommasi, G. *Ann. N. Y. Acad. Sci*. **2003**, *984*, 226.
(65) Paddison, S. J. First principles modeling of sulfonic acid based ionomer membranes. In *Handbook of Fuel Cells − Fundamentals, Technology and Applications Volume 3 − Fuel Cell Technology and Applications*; Vielstich, W., Lamm, A., Gasteiger, H., Eds.; J. Wiley and Sons: Chichester, UK, 2003.
(66) Johansson, P.; Tegenfeldt, J.; Lindgren, J. *Electrochim. Acta* **2000**, *45*, 3055.
(67) Vishnyakov, A.; Neimark, A. V. *J. Phys. Chem. B* **2000**, *104*, 4471.
(68) Vishnyakov, A.; Neimark, A. V. *J. Phys. Chem. B* **2001**, *105*, 7830.
(69) Elliott, J. A.; Hanna, S.; Elliott, A. M. S.; Cooley, G. E. *Macromolecules* **2000**, *33*, 4161.

(70) Li, T.; Wlaschin, A.; Balbuena, P. B. *Ind. Eng. Chem. Res.* **2001**, *40*, 4789.
(71) Eikerling, M.; Kornyshev, A. A. *J. Electroanal. Chem.* **2001**, *502*, 1.
(72) Eikerling, M.; Kornyshev, A. A.; Kuznetsov, A. M.; Ulstrup, J.; Walbran, S. *J. Phys. Chem. B* **2001**, *105*, 3646.
(73) Spohr, E.; Commer, P.; Kornyshev, A. A. *J. Phys. Chem. B* **2002**, *106*, 10560.
(74) Commer, P.; Cherstvy, A. G.; Spohr, E.; Kornyshev, A. A. *Fuel Cells* **2002**, *2*, 127.
(75) Spohr, E. *Mol. Simul.* **2004**, *30*, 107.
(76) Yang, Y.; Pintauro, P. N. *Ind. Eng. Chem. Res.* **2004**, *43*, 2957.
(77) Jang, S. S.; Molinero, V.; Cagin, T.; Goddard, W. A. *J. Phys. Chem. B* **2004**, *108*, 3149.
(78) Petersen, M. K.; Wang, F.; Blake, N. P.; Metiu, H.; Voth, G. A. *J. Phys. Chem. B* **2005**, *109*, 3727.
(79) Choi, P.; Jalani, N. H.; Datta, R. *J. Electrochem. Soc.* **2005**, *152*, E123.
(80) Khalatur, P. G.; Talitskikh, S. K.; Khokhlov, A. R. *Macromol. Theory Simul.* **2002**, *11*, 566.
(81) Paddison, S. J.; Pratt, L. R.; Zawodzinski T.; Reagor, D. W. *Fluid Phase Equilib.* **1998**, *150*−*151*, 235.
(82) Paddison, S. J.; Pratt, L. R.; Zawodzinski Jr. T. A. In *Proton Conducting Membrane Fuel Cells II, 98*−*27*; Gottesfeld, S., Fuller, T. F., Eds.; The Electrochemical Society Proceedings Series; The Electrochemical Society: Pennington, NJ, 1999; pp 99−105.
(83) Paddison, S. J.; Zawodzinski Jr. T. A. *Solid State Ionics* **1998**, *113*−*115*, 333.
(84) Paddison, S. J.; Pratt, L. R.; Zawodzinski, T. A., Jr. *J. New Mater. Electrochem. Sys.* **1999**, *2*, 183.
(85) Paddison, S. J.; Pratt, L. R.; Zawodzinski, T. A., Jr. *J. Phys. Chem. A* **2001**, *105*, 6266.
(86) Paddison, S. J. *J. New Mater. Electrochem. Sys.* **2001**, *4*, 197.
(87) Eikerling, M.; Paddison, S. J.; Zawodzinski, T. A., Jr. *J. New Mater. Electrochem. Sys.* **2002**, *5*, 15.
(88) Paddison, S. J.; Paul, R.; Zawodzinski, T. A., Jr. In *Proton Conducting Membrane Fuel Cells II, 98*−*27*, Gottesfeld, S., Fuller, T. F., Eds.; The Electrochemical Society Proceedings Series; The Electrochemical Society: Pennington, NJ, 1999; pp 106−120.
(89) Paddison, S. J.; Paul, R.; Zawodzinski, T. A., Jr. *J. Electrochem. Soc.* **2000**, *147*, 617.
(90) Paddison, S. J.; Paul, R.; Zawodzinski, T. A., Jr. *J. Chem. Phys.*, **2001**, *115*, 7753.
(91) Paddison, S. J.; Paul, R.; Pivovar, B. S. In *Direct Methanol Fuel Cells, 01*−*04*; Narayanan, S., Gottesfeld, S., Zawodzinski, T. A., Eds.; The Electrochemical Society Proceedings Series; The Electrochemical Society: Pennington, NJ; 2001; pp 8−13.
(92) Paddison, S. J.; Paul, R.; Kreuer, K. D.; Zawodzinski, T. A., Jr. In *Direct Methanol Fuel Cells, 01*−*04*; Narayanan, S., Gottesfeld, S., Zawodzinski, T. A., Eds.; The Electrochemical Society Proceedings Series; The Electrochemical Society: Pennington, NJ; 2001; pp 29−33.
(93) Paddison, S. J.; Paul, R.; Kreuer, K. D. *Phys. Chem. Chem. Phys.* **2002**, 4, 1151.
(94) Paddison, S. J.; Paul, R. *Phys. Chem. Chem. Phys.* **2002**, *4*, 1158.
(95) Paul, R.; Paddison, S. J. In *Advances in Materials Theory and Modeling* − *Bridging Over Multiple-Length and Time Scales*; Bulatov, V., Colombo, L., Cleri, F., Lewis, L. J., Mousseau, N., Eds.; Materials Research Society: Warrendale, PA, 2001.
(96) Paul, R.; Paddison, S. J. *J. Chem. Phys.* **2001**, *115*, 7762.
(97) Paul, R.; Paddison, S. J. *Phys. Rev. E* **2003**, *67*, 016108.
(98) Paul, R.; Paddison, S. J. *Solid State Ionics* **2004**, *168*, 245.
(99) Paul, R.; Paddison, S. J. *J. Phys. Chem. B* **2004**, *108*, 13231.
(100) Paddison, S. J.; Reagor, D. W.; Zawodzinski, T. A. *J. Electroanal. Chem.* **1998**, *459*, 91.
(101) Paddison, S. J.; Bender, G.; Kreuer, K. D.; Nicoloso, N.; Zawodzinski Jr., T. A. *J. New Mater. Electrochem. Systems* **2000**, **3**, 291.
(102) Frisch, M. J.; Trucks, G. W.; Schlegel, H. B.; Scuseria, G. E.; Robb, M. A.; Cheeseman, J. R.; Montgomery, J. A., Jr.; Vreven, T.; Kudin, K. N.; Burant, J. C.; Millam, J. M.; Iyengar, S. S.; Tomasi, J.; Barone, V.; Mennucci, B.; Cossi, M.; Scalmani, G.; Rega, N.; Petersson, G. A.; Nakatsuji, H.; Hada, M.; Ehara, M.; Toyota, K.; Fukuda, R.; Hasegawa, J.; Ishida, M.; Nakajima, T.; Honda, Y.; Kitao, O.; Nakai, H.; Klene, M.; Li, X.; Knox, J. E.; Hratchian, H. P.; Cross, J. B.; Adamo, C.; Jaramillo, J.; Gomperts, R.; Stratmann, R. E.; Yazyev, O.; Austin, A. J.; Cammi, R.; Pomelli, C.; Ochterski, J. W.; Ayala, P. Y.; Morokuma, K.; Voth, G. A.; Salvador, P.; Dannenberg, J. J.; Zakrzewski, V. G.; Dapprich, S.; Daniels, A. D.; Strain, M. C.; Farkas, O.; Malick, D. K.; Rabuck, A. D.; Raghavachari, K.; Foresman, J. B.; Ortiz, J. V.; Cui, Q.; Baboul, A. G.; Clifford, S.; Cioslowski, J.; Stefanov, B. B.; Liu, G.; Liashenko, A.; Piskorz, P.; Komaromi, I.; Martin, R. L.; Fox, D. J.; Keith, T.; Al-Laham, M. A.; Peng, C. Y.; Nanayakkara, A.; Challacombe, M.; Gill, P. M. W.; Johnson, B.; Chen, W.; Wong, M. W.; Gonzalez, C.; Pople, J. A., Gaussian 03, Revision C.02, Gaussian, Inc., Wallingford CT, 2004.
(103) Schlegel, H. B. *J. Comput. Chem.* **1982**, *3*, 214.
(104) Hariharan, P. C.; Pople, J. A. *Theor. Chim. Acta* **1973**, *28*, 213.
(105) Becke, A. D. *J. Chem. Phys.* **1993**, *98*, 5648.
(106) Becke, A. D. *J. Chem. Phys.* **1993**, *98*, 1372.
(107) Lee, C. T.; Yang, W. T.; Parr, R. G. *Phys. Rev. B* **1998**, *37*, 785.
(108) McLean, A. D.; Chandler, G. S. *J. Chem. Phys.* **1980**, *72*, 5639.
(109) Boys, S. F.; Bernardi, F. *Mol. Phys.* **1970**, *19*, 55.
(110) Donaldson, D. J. *J. Phys. Chem. A* **1999**, *103*, 62.
(111) Kobko, N.; Dannenberg, J. J. *J. Phys. Chem. A* **2001**, *105*, 1944.
(112) Tzeli, D.; Mavridis, A.; Xantheas, S. S. *Chem. Phys. Lett.* **2001**, *340*, 538.
(113) Garza, J.; Ramírez, J. Z.; Vargas, R. *J. Phys. Chem. A* **2005**, *109*, 643.
(114) Chesnut, D. B. *J. Phys. Chem. A* **2002**, *106*, 6876.
(115) Salvador, P.; Duran, M.; Dannenberg, J. J. *J. Phys. Chem. A* **2002**, *106*, 6883.